Electron Paramagnetic Resonance Study on ^{28}Si Single Crystal for the Future Realization of the Kilogram

Shigeki Mizushima, Naoki Kuramoto, Kenichi Fujii, and Takahide Umeda

***Abstract*— For the future realization of the kilogram using the X-ray crystal density (XRCD) method, isotopically enriched silicon crystals grown by the floating zone method are employed. In this paper, we present quantitative electron paramagnetic resonance (EPR) measurements on ^{28}Si single crystal AVO28 to increase the reliability of mass deficit correction in the XRCD method. We detected phosphorus impurity in the crystal and determined its concentration to be 3.2(5) × 10^{12} cm^{-3}, which is consistent with that estimated using Fourier transform infrared spectroscopy. In addition, the EPR measurements revealed that the concentrations of nine types of vacancy defects with unpaired electrons in the crystal are less than 1 × 10^{12} cm^{-3} at 25 K both in a dark environment and under illumination. As a result, the necessary mass deficit correction due to these vacancy defects is estimated to be 0.0(2) μg for 1-kg AVO28 spheres.**

***Index Terms*— Electron paramagnetic resonance (EPR), kilogram, measurement uncertainty, metrology, silicon crystal, vacancy defects.**

I. Introduction

THE X-ray crystal density (XRCD) method is one of two independent methods that can realize the future realization of the kilogram with the highest accuracy [1]. The mass of a ^{28}Si single-crystal sphere with a diameter of approximately 93.7 mm is determined by counting the number of silicon atoms in the sphere along with using several basic physical constants, including the Planck constant h. If a significant number of defects exist in the crystal, then the mass deficit caused by their presence must be corrected. Here, the mass deficit is defined as the mass difference between two silicon spheres with a diameter of 93.7 cm, one of which is made of an ideal crystal, and the other of which is made of a real crystal containing defects. Fig. 1 shows the schematic of a normal structure, monovacancy defect V, and substitutional impurity defect in silicon crystals.

Manuscript received June 26, 2018; revised October 16, 2018; accepted November 8, 2018. Date of publication December 17, 2018; date of current version May 10, 2019. This work was supported by JSPS KAKENHI under Grant 17K05112. The Associate Editor coordinating the review process was Dr. Michael Lombardi. *(Corresponding author: Shigeki Mizushima.)*

S. Mizushima, N. Kuramoto, and K. Fujii are with the National Metrology Institute of Japan, National Institute of Advanced Industrial Science and Technology, Tsukuba 305-8563, Japan (e-mail: s.mizushima@aist.go.jp; n.kuramoto@aist.go.jp; fujii.kenichi@aist.go.jp).

T. Umeda is with Institute of Applied Physics, University of Tsukuba, Tsukuba 305-8573, Japan (e-mail: umeda@bk.tsukuba.ac.jp).

Color versions of one or more of the figures in this paper are available online at http://ieeexplore.ieee.org.

Digital Object Identifier 10.1109/TIM.2018.2884044

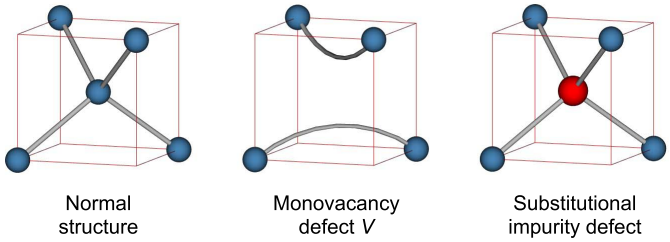

Fig. 1. Ball-and-stick models of a normal structure, monovacancy defect V, and substitutional impurity defect in silicon crystals. Gray lines: chemical bonds between atoms.

Several studies on defects in silicon crystals have been conducted to realize the kilogram using silicon crystals. Deslattes and Kessler [2] reported a qualitative difference between a silicon crystal with a natural isotope ratio of National Metrology Institute of Japan (NMIJ), formerly National Research Laboratory of Metrology, and that of Physikalisch-Technische Bundesanstalt by employing electron paramagnetic resonance (EPR) spectroscopy. They detected the EPR signals of impurities only from the NMIJ's crystal. Gebauer *et al.* [3] determined that the vacancy concentration in a silicon crystal grown by the floating zone (FZ) method ranges from 1 × 10^{14} cm^{-3} to 4 × 10^{14} cm^{-3} using positron annihilation lifetime spectroscopy (PALS) that detects neutral or negatively charged vacancies. They performed electron irradiation with low doses to obtain a quantitative calibration using an estimated introduction rate of 0.1 cm^{-1} for monovacancies. They did not find any relation between the average positron lifetime and the position in the radial direction of the crystal. They concluded that a decomposition of the positron lifetime spectra does not give reliable results because of the low intensities of the defect components. They estimated that hexavacancy V_6 is a candidate for explaining their PALS results. D'Agostino *et al.* [4] developed a method to measure the void concentration of 10^{14} cm^{-3} in a silicon crystal with a few percent uncertainties using Cu decoration and neutron activation.

At present, the International Avogadro Coordination (IAC) project estimates a vacancy defect concentration of 3.3(1.1) × 10^{14} cm^{-3} in ^{28}Si crystals grown by the FZ method, which was determined using PALS [5]. The IAC considers that this value represents the vacancy content per unit volume for all vacancy types including vacancy agglomerates and voids, which is expressed as $\sum_n nc(V_n)$,

where n is the vacancy size ($n = 1$ for monovacancy V, $n = 2$ for divacancy V_2, $n = 3$ for trivacancy V_3, etc.), and $c(V_n)$ is the concentration of the vacancy V_n. The value $3.3(1.1) \times 10^{14}$ cm^{-3} corresponds to a mass deficit correction of 6.6(2.2) μg for a 1-kg ^{28}Si sphere. To confirm the reliability of this value, it is desirable to perform further measurements using other independent methods.

To date, a lot of detailed studies on vacancy defects in silicon crystals have been conducted using EPR spectroscopy [6], which is one of the high-sensitivity methods for identifying and quantifying vacancy defects. This paper reports the quantitative EPR measurement on ^{28}Si single crystal AVO28 to increase the reliability of mass deficit correction in the XRCD method. This paper is the extension of a presentation at the 2018 Conference on Precision Electromagnetic Measurements (CPEM 2018) and a two-page summary published in the CPEM 2018 Digest [7].

This paper proceeds as follows. Section II describes the defect concentration measurement method using EPR spectroscopy. Section III shows the preparation of a sample cut out from the AVO28 crystal. Section IV describes the measurement results using EPR spectroscopy. Section V discusses the measurement results obtained. Finally, Section VI presents the conclusions of this paper.

II. Measurement Method

EPR spectroscopy detects unpaired electrons localized at defects such as vacancies and impurities in a sample. EPR spectra are recorded by irradiating the sample placed in a microwave cavity resonator with the microwave (frequency ν) and sweeping an external magnetic field B. Resonant microwave absorptions (i.e., EPR signals) are observed under the resonance condition, where the energy of a microwave photon is equal to the Zeeman splitting of the energy levels of an unpaired electron

$$h\nu = g\mu_B B \tag{1}$$

where h is the Planck constant, g is the gyromagnetic factor (g-factor) of the unpaired electron, and μ_B is the Bohr magneton. The g-factor for free electrons has been determined to be $2.002\,319\cdots$ with a relative standard uncertainty of 2.6×10^{-13} [8]. The g-factor of the electron localized at a defect has an inherent deviation caused by spin-orbit coupling. Therefore, measurements of the g-factor are useful for classifying defects.

Furthermore, since the wave function of the unpaired electron has a spatial distribution reflecting the arrangement of atoms around a defect, the angular dependence of the g-factor provides information on the symmetry of the defect in a crystal sample. By choosing a particular Cartesian coordinate system, the effective value of the g-factor for the defect in a certain direction g_{eff} is given by

$$g_{\text{eff}} = \left(g_x^2 \cos^2\theta_x + g_y^2 \cos^2\theta_y + g_z^2 \cos^2\theta_z\right)^{1/2} \tag{2}$$

where g_x, g_y, and g_z are the principal values of the g-factor and $\cos\theta_x$, $\cos\theta_y$, and $\cos\theta_z$ are the direction cosines of the magnetic field in the selected Cartesian coordinate system.

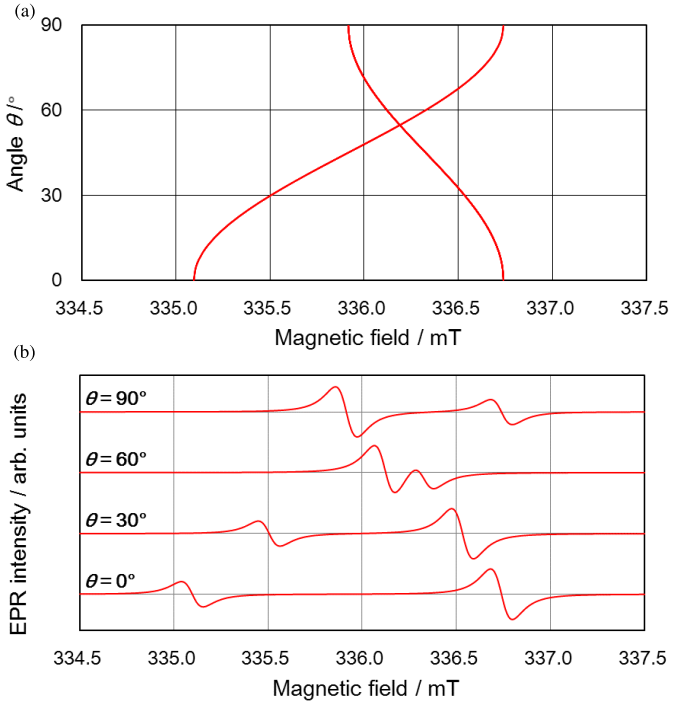

Fig. 2. Simulation results of the anisotropic EPR signal of the positively charged monovacancy defect V^+ with the principal values of $g_x = 2.0087(3)$, $g_y = 1.9989(3)$, and $g_z = 1.9989(3)$ [11]. This defect shows axial symmetry about the <100> direction of the crystal. (a) Angular dependence of EPR line positions. Angle θ: angle between the [100] direction of the silicon single crystal and the magnetic field rotating in the $(0\bar{1}1)$ plane. (b) First-derivative EPR spectra for $\theta = 0°$, 30°, 60°, and 90°. For this simulation, a microwave frequency of 9.421 GHz and Lorentzian lineshapes with a half-width at half-maximum $\Gamma = 0.1$ mT was assumed. In an EPR spectrum, multiple EPR lines appear depending on the direction of the magnetic field owing to the rotational symmetry of the crystal. Taking into account the symmetry of the silicon crystal, the maximum number of EPR lines observed is 12.

When the arrangement of atoms around the defect has cubic symmetry such as tetrahedral group T_d, all three principal values of the g-factor are equal and such an EPR signal is expressed as "isotropic." Otherwise, the EPR signal is referred to as "anisotropic."

Watkins [6] identified anisotropic EPR signals of vacancy defects in silicon crystals, generated by high-energy electron irradiation. The principal values of the g-factor range from 1.9989 to 2.0087 for positively charged monovacancy defect V^+ and from 2.0028 to 2.0151 for negatively charged monovacancy defect V^-. Such anisotropy of EPR signals is caused by the geometrical distortion of the four silicon atoms around a vacancy defect due to the Jahn–Teller effect [9].

In addition, charged divacancy, trivacancy, tetravacancy, and pentavacancy defects $V_2^{\pm}$, V_3^-, V_4^-, and V_5^- and monovacancy defects trapped by impurities $(VO)^-$ and $(VP)^0$ in silicon crystals have been identified by EPR spectroscopy [6], [10]. These anisotropic signals of the vacancy defects should appear in the magnetic field ranging from 334 to 337 mT at the microwave frequency of 9.421 GHz used in our study. Fig. 2 shows the simulation results of anisotropic EPR signals of the positively charged monovacancy defect V^+ in a silicon single crystal [11] as an example, which is available using the web-based database system [12].

The angular dependence of the EPR signals observed for irradiation-damaged silicon crystals is explained by the geometrical distortion of atoms around each type of vacancy, based on the Jahn–Teller effect. Because the atoms around the vacancy in undamaged silicon crystals should have the geometrical distortion similar to that of the irradiation-damaged silicon crystals, based on the Jahn–Teller effect, we believe that the identification performed on irradiation-damaged samples using EPR is applicable to undamaged samples used in this paper.

Among the 415 types of defects in silicon identified in previous EPR studies [13], the largest vacancy agglomerate is negatively charged pentavacancy defect V_5^- [14]. On the other hand, to the best of our knowledge, the largest vacancy agglomerate estimated using PALS is hexavacancy defect V_6 in an electron-irradiated FZ silicon doped with phosphorus for an estimated positron lifetime of 400 ps [15].

Furthermore, when the wave function of an unpaired electron spreads to the position of an impurity atom having nuclear spin I, where I is an integer or half-integer, the EPR signal splits into $(2I + 1)$ lines owing to the hyperfine interaction. Since the number of lines and splitting width of the hyperfine splitting depend on the impurity atom and the wave function of the unpaired electron, they are useful for identifying impurity defects.

The ^{28}Si single crystal used in this paper contains ^{29}Si atoms, which have a nuclear spin $I = 1/2$, with an amount-of-substance fraction of only 4×10^{-5} [16]. This brings about relatively narrow line widths of the EPR signals and makes it possible to acquire high-resolution EPR spectra. This is a great advantage in determining a small amount of vacancy defect concentration compared to the measurement on silicon crystals with a natural isotope ratio, which contains ^{29}Si atoms with an amount-of-substance fraction of approximately 0.047, causing inhomogeneous broadening in the EPR signals owing to the hyperfine interaction.

Quantitative determination of the number of EPR-active defects can be achieved through comparison with a reference sample with a known number of unpaired electrons. This is based on the measurement principle that each EPR absorption intensity is proportional to the number of unpaired electrons in a sample. When we use the reference sample with the number of unpaired electrons n_R, the number of unpaired electrons localized at a certain type of defect X in the test sample n_X, is given by

$$n_X = \left(\frac{A_X}{A_R}\right)\left(\frac{T_X}{T_R}\right) n_R \tag{3}$$

where (A_X/A_R) is the ratio of the EPR absorption intensities for the test and reference samples and (T_X/T_R) is the ratio of the absolute temperatures of the test and reference samples being measured. Here, we used Curie's law, which states that the magnetization of the paramagnetic material is approximately inversely proportional to the absolute temperature.

The concentration of defect X with an unpaired electron in the test sample c_X is obtained by dividing the number of unpaired electrons localized at the defect n_X by a sample volume V_s

$$c_X = n_X / V_s. \tag{4}$$

We used a crystal of copper(II) sulfate pentahydrate $CuSO_4{\cdot}5H_2O$ (molar mass $M = 249.69$ g mol^{-1}) with a mass of 12.53 mg as the reference sample, which retains one unpaired electron per molecule. The number of unpaired electrons in the reference sample n_R was estimated to be $3.02(3) \times 10^{19}$. The EPR absorption intensity of the reference sample A_R was determined at $T_R = 298$ K before measurements on the test sample using the same instrument.

All EPR measurements were carried out using a Bruker Bio-Spin E500 X-band spectrometer equipped with a super-high-Q cavity ER 4122SHQ. The signal-to-noise ratio of the instrument is 3000 for the paramagnetic radical standard material, called weak pitch, having a linear density of unpaired electrons of around 10^{13} cm^{-1}. The detectable minimum number of unpaired electrons in the sample placed in the microwave cavity resonator was estimated to be around 10^{10}, which is ultimately limited by the thermal noise of the detector and amplifiers [17]. The quality factor of the microwave cavity resonator Q reaches 7500 under the best measurement conditions. The sample temperature was controlled from 4 K to room temperature using an Oxford ESR900 He-flow cryostat. Standard magnetic field modulation technique was employed at a frequency of 100 kHz with a modulation width of 0.1 mT.

In quantitative EPR measurements, it is necessary to avoid microwave saturation that causes the underestimation of EPR signal intensities. Without microwave saturation, the intensity of any EPR signal should be proportional to the square root of the microwave power. Therefore, the intensity of the EPR signal was examined beforehand at four microwave powers of 0.002, 0.02, 0.2, and 2 mW.

Furthermore, out-of-phase second-harmonic EPR signals under rapid-passage conditions [18] were observed to selectively detect defects with long electron spin relaxation times in the sample. It was found that the concentrations of defects with long electron spin relaxation times were below the detection limit of our measurement in the expected magnetic field range from 334 to 337 mT for the EPR-active vacancy defects.

III. Sample Preparation

The sample for EPR spectroscopy was prepared from semicircular disk-shaped sample 9.R1, cut out from the tail side of ^{28}Si single-crystal Si28-10Pr11 (referred to as AVO28) [5]. The sample has a rectangular solid shape with the dimensions of 1.8 mm × 3.4 mm × 10.4 mm. The axial distance between the sample and the seed of the AVO28 crystal was approximately 420 mm, and the radial distance from the center was approximately 35 mm. The dimensions of the sample were designed by taking into account the internal dimensions of the microwave cavity resonator and the distribution of the microwave field B_1 in the microwave cavity resonator. The volume of the sample at 20 °C was determined to be $V_s = 0.065\ 029(5)$ cm^3 from the crystal density [16] and the mass measured using a vacuum mass comparator [19]. Fig. 3 shows a photograph of the sample and the crystal orientations.

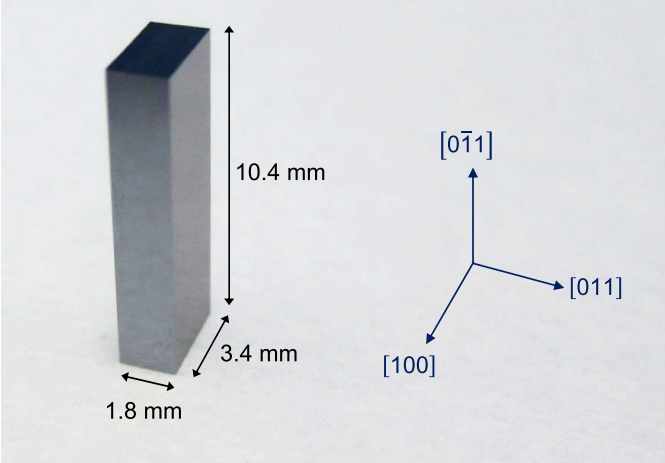

Fig. 3. Photograph of the mirror-polished crystal prepared from semicircular disk-shaped sample 9.R1, cut out from the tail side of the AVO28 crystal. The indices on the right side indicate the crystal orientations.

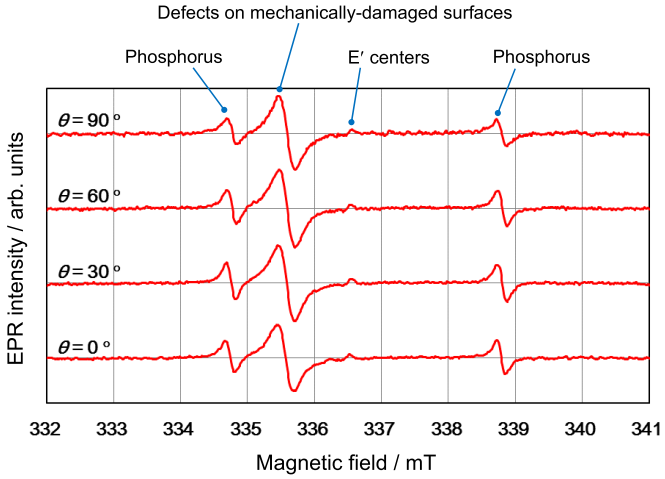

Fig. 4. First-derivative EPR spectra of the AVO28 crystal sample under illumination. To investigate angular dependence, the sample was rotated about the [0$\bar{1}$1] direction. Angle θ: angle between the magnetic field and the [100] direction. Each spectrum is accumulated for 3.7 h to improve the signal-to-noise ratio. These spectra were measured without microwave saturation for phosphorus impurity and defects on mechanically damaged surfaces at a microwave power of 2 mW.

To detect a small EPR signal from the bulk crystal, we must reduce the EPR signals of defects near the sample surfaces, which were formed during the manufacturing process. For this purpose, the surface area of 1.09 cm^2, out of the total surface area of 1.21 cm^2, was mirror polished. Half of the remaining surface is the as-etched surface, and the other half is the as-cut surface finished using a dicing saw. From our experience, the silicon surface, properly cut using a dicing saw, is almost equivalent to the mirror-polished surface in terms of the surface density of dangling bonds. After our EPR measurement, it became apparent that chemical etching is necessary to minimize the dangling bond density on the sample surfaces.

The sample surfaces were then precisely cleaned to reduce the signal of the surface contaminants. The cleaning was conducted in four cleaning steps by successively using the following solutions: sulfuric acid peroxide mixture, ammonia peroxide mixture, hydrogen chloride peroxide mixture, and diluted hydrofluoric acid.

IV. Measurement Results

To detect vacancy defects in the sample, EPR measurements were conducted in the presence of a magnetic field from 332 to 341 mT. EPR spectra were recorded at four different directions $\theta = 0°$, 30°, 60°, and 90° by rotating the sample about the [0$\bar{1}$1] direction, where θ represents the angle between the magnetic field and the [100] direction. Fig. 4 shows the first-derivative EPR spectra under 100-W halogen lamp illumination at 25 K. The halogen lamp illumination generates a large number of electron–hole pairs in the silicon crystal sample, provides additional unpaired electrons, and reveals the defects that cannot be observed in a dark environment. To guide light from the halogen lamp to the sample, a quartz glass rod, on which the sample was mounted, was employed.

Electron–hole pairs excited near the sample surfaces under illumination spread into all parts of the sample. The reason for this is that the minority carrier diffusion length $L = (\tau D)^{1/2}$ is estimated to be greater than a silicon sample thickness of 1.8 mm. Here, τ is the minority carrier lifetime in silicon crystals and D is the diffusion coefficient of carriers in silicon crystals. If we use a value of the minority carrier lifetime $\tau = 21.6$ ms [20] and a value of the diffusion coefficient of carriers $D = 350$ cm^2 s^{-1} for electrons at 25 K [21], the minority carrier diffusion length is estimated at 27 mm.

The observed EPR spectra identified the following three types of defects.

1) *Phosphorus (^{31}P, Nuclear Spin $I = 1/2$) Impurity:* The constituent element is represented by $Si_4 \equiv P\bullet$, where the lines symbolize chemical bonds and the dot symbolizes an unpaired electron. Phosphorus is a typical substitutional impurity in the silicon crystal. The identification is based on the facts that the spectra show a doublet hyperfine splitting of 4.04 mT owing to a ^{31}P hyperfine interaction, and the g-value of the spectral center is 1.9990(1) and isotropic, which are in good agreement with the well-established EPR signal of phosphorus donors in silicon crystal [22], [23]. This isotropic signal results from the tetrahedral symmetric structure, where four silicon atoms bond to a phosphorus atom without geometric distortion. The observed linewidth of the spectra was $2\Gamma = 0.24$ mT.

   The number and concentration of the phosphorus impurity with unpaired electrons under illumination are determined to be $0.21(3) \times 10^{12}$ and $3.2(5) \times 10^{12}$ cm^{-3}, respectively, based on (3) and (4). Table I shows the numerical values used for this determination and its uncertainty evaluation. The phosphorus EPR signal fell below the detection limit in a dark environment. This indicates that unpaired electrons of the phosphorus donors transferred to other compensating defects in the sample in a dark environment ($Si_4 \equiv P \bullet \rightarrow Si_4 \equiv P + \bullet$). This is known as a "compensation"

TABLE I
UNCERTAINTY EVALUATION OF CONCENTRATION OF PHOSPHORUS IMPURITY WITH UNPAIRED ELECTRONS UNDER ILLUMINATION

Uncertainty component	Value	Relative standard uncertainty
EPR absorption intensity from the test sample, A_X	0.74 arb. units	0.06
EPR absorption intensity from the reference sample, A_R	8.8919×10^6 arb. units	0.06
Absolute temperature of the test sample, T_X	25 K	0.02
Absolute temperature of the reference sample, T_R	298 K	0.004
Number of unpaired electrons in the reference sample, n_R	3.022×10^{19}	0.01
Difference in shape between reference and test samples in nonuniform microwave magnetic field B_1		0.06
Difference in position between reference and test samples in nonuniform microwave magnetic field B_1		0.06
Difference in transmission medium between reference and test samples for microwave magnetic field B_1		0.06
Significant difference in temperature between reference and test samples		0.06
Number of phosphorus atoms with unpaired electrons in the test sample, n_X	0.21×10^{12}	0.14

Uncertainty component	Value	Relative standard uncertainty
Number of phosphorus atoms with unpaired electrons in the test sample, n_X	0.21×10^{12}	0.14
Volume of the test sample at 20 °C, V_s	0.0650 cm^3	8×10^{-5}
Concentration of phosphorus atoms with unpaired electrons in the test sample, c_X	3.2×10^{12} cm^{-3}	0.14

phenomenon, namely, a decrease in the number of charge carriers in a semiconductor material, which contains both donors and acceptors. We suggest that such compensating defects originate from boron impurity with a relatively high concentration at the tail of the AVO28 crystal and also from the defects on mechanically damaged surfaces described in the following.

2) *Defects Formed Near the Mechanically-Damaged Surfaces of Silicon Single Crystal* ($Si_3 \equiv Si\bullet$): The identification is based on the result that the g-value of the observed spectral center is close to 2.0055(2) [24] and isotropic. Most of these defects may be formed at microcracks near the as-cut surface with a surface area of 0.06 cm^2, finished using a dicing saw or mirror-polished surfaces. The linewidth of the spectra on the ^{28}Si single crystal used in this paper is $2\Gamma = 0.41$ mT, which is clearly narrower than that reported for natural isotope ratio crystals of 0.7–0.8 mT [24].

The number of EPR-active defects on the mechanically damaged surfaces was determined to be $1.67(23) \times 10^{12}$ in a dark environment and $0.68(10) \times 10^{12}$ under illumination. They are larger than the number of phosphorous impurity defects observed under illumination, $0.21(3) \times 10^{12}$. We judge that unpaired electrons of phosphorus impurities acting as donors move to defects on the mechanically damaged surfaces, hiding the EPR signals of phosphorus in a dark environment. Under illumination, some of the unpaired electrons at defects on the mechanically damaged surfaces transfer to phosphorus impurity defects, thus recovering the EPR-active state ($Si_4 \equiv P + \bullet \rightarrow Si_4 \equiv P\bullet$).

3) E' centers ($O_3 \equiv Si\bullet$), oxygen-vacancy defects in the quartz glass rod, on which the sample was mounted. The identification is based on the observation of isotropic and easily saturable signals with average g-value close to 2.0008 [25]. The microwave saturation

TABLE II
CONCENTRATIONS OF NINE TYPES OF VACANCY DEFECTS WITH UNPAIRED ELECTRONS AND THE CORRESPONDING MASS DEFICITS FOR A 1-kg ^{28}Si SINGLE CRYSTAL

Types of vacancy defect with an unpaired electron	Concentration /(10^{12} cm^{-3})	Mass deficit for a 1 kg ^{28}Si single crystal, δm/μg
V^+	0.0(6)	0.00(1)
V^-	0.0(6)	0.00(1)
V_2^+	0.0(6)	0.00(2)
V_2^-	0.0(6)	0.00(2)
V_3^-	0.0(6)	0.00(3)
V_4^-	0.0(6)	0.00(5)
V_5^-	0.0(6)	0.00(6)
$(VO)^-$	0.0(6)	0.00(1)
$(VP)^0$	0.0(6)	0.00(1)
Total	0.0(5.2)	0.00(23)

For conversion from concentration of vacancy defects to the mass deficit, a number density of ^{28}Si atoms in a single crystal at 20 °C of approximately 4.99×10^{22} cm^{-3} was used.

occurred even at a microwave power of 0.02 mW. This signal is detectable without the silicon sample and is irrelevant to the silicon sample.

However, anisotropic EPR signals of the vacancy defects were not observed in the expected magnetic field range of 334 to 337 mT under illumination. This result indicates that the concentrations of nine types of vacancy defects with unpaired electrons V^+, V^-, V_2^+,V_2^-,V_3^-,V_4^-,V_5^-, $(VO)^-$, and $(VP)^0$, which were previously identified by Watkins [6] and Lee and Corbett [10] using EPR spectroscopy, are all below the detection limit of our EPR measurement, estimated as around 1×10^{12} cm^{-3}. This value of the detection limit was estimated from the fact that the signals of the phosphorus impurity with unpaired electrons having a concentration of $3.2(5) \times 10^{12}$ cm^{-3}, which split into two spectra, are clearly distinguished from background noise, as shown in Fig. 4. Similar EPR measurement conducted in a dark environment also revealed that anisotropic EPR signals of the vacancy defects were below the detection limit of our measurement.

Table II shows the evaluated concentrations of the nine types of vacancy defects with unpaired electrons and the corresponding mass deficits for a 1-kg ^{28}Si single crystal. Each concentration of vacancy defects with unpaired electrons is estimated to be 0.0×10^{12} cm^{-3}. The standard uncertainty is estimated to be 0.6×10^{12} cm^{-3}, assuming a uniform distribution with a half-width of 1×10^{12} cm^{-3}, which is the estimated detection limit of our EPR measurements. The total mass deficit due to vacancy defects with unpaired electrons δm is estimated to be 0.00(23) μg for a 1-kg ^{28}Si single crystal using the following equation:

$$\delta m = \delta m_{V^+} + \delta m_{V^-} + \delta m_{V_2^+} + \delta m_{V_2^-} + \delta m_{V_3^-} + \delta m_{V_4^-} + \delta m_{V_5^-} + \delta m_{(VO)^-} + \delta m_{(VP)^0} \quad (5)$$

where $\delta m_{V^+}, \delta m_{V^-}, \cdots, \delta m_{(VP)^0}$ represent a mass deficit due to each type of vacancy defect.

The vacancy concentrations estimated in this paper are limited to those for the nine types of vacancy defects in silicon crystals, as identified in previous EPR studies. Therefore, it should be noted that the mass deficit estimated in this paper corresponds only to these nine types of vacancy defects.

The standard uncertainty of the total mass deficit due to vacancy defects with unpaired electrons $u(\delta m)$ is given by

$$u(\delta m) = u(\delta m_{V^+}) + u(\delta m_{V^-}) + u(\delta m_{V_2^+}) + u(\delta m_{V_2^-}) + u(\delta m_{V_3^-}) + u(\delta m_{V_4^-}) + u(\delta m_{V_5^-}) + u(\delta m_{(VO)^-}) + u(\delta m_{(VP)^0}) \quad (6)$$

where $u(\delta m_{V^+}), u(\delta m_{V^-}), \cdots, u(\delta m_{(VP)^0})$ are the standard uncertainties of mass deficits $\delta m_{V^+}, \delta m_{V^-}, \cdots, \delta m_{(VP)^0}$. In this estimation, we assume that correlation coefficients between the mass deficits are +1.

V. DISCUSSION

The sample cut out from ^{28}Si single crystal AVO28 was measured at 25 K using EPR spectroscopy. Under illumination, the number and concentration of EPR-active phosphorus

impurity ($Si_4 \equiv P\bullet$) in the sample were determined to be $0.21(3) \times 10^{12}$ and $3.2(5) \times 10^{12}$ cm^{-3}, respectively. In a dark environment, the number of EPR-active defects on the mechanically damaged surfaces ($Si_3 \equiv Si\bullet$) was determined to be $1.67(23) \times 10^{12}$. The clear observations of low concentrations of phosphorous impurity and defects on mechanically damaged surfaces demonstrate that EPR measurements used in this paper have adequate sensitivity to vacancy defects at a concentration of 1×10^{12} cm^{-3}.

The concentration of phosphorus impurity obtained in this paper, $3.2(5) \times 10^{12}$ cm^{-3}, agrees with that of sample 4.12 of the AVO28 crystal shown in [26, Table 3], $10(10) \times 10^{12}$ cm^{-3}, which was estimated from measurement results using Fourier transform infrared (FTIR) spectroscopy for ^{28}Si crystal Si28-23Pr11. It is worth noting that the phosphorus impurity in the silicon crystal serves as a common scale for EPR and FTIR measurements.

The measured surface density of defects on the mechanically damaged surfaces gives a value of $1.67(23) \times 10^{12}$ / $1.21(2)$ cm^2 $= 1.4(2) \times 10^{12}$ cm^{-2}. This value is comparable to that of hydrogenated amorphous silicon (a-Si:H) films, determined using photothermal deflection spectroscopy, around 10^{12} cm^{-2} [27].

On the other hand, anisotropic signals of nine types of vacancy defects were not observed in the expected magnetic field ranging from 334 to 337 mT both in a dark environment and under illumination. The concentrations of the nine types of vacancy defects were estimated to be $0.0(6) \times 10^{12}$ cm^{-2}, respectively. Consequently, the mass deficit correction for these vacancy defects is evaluated to be 0.0(2) μg for a 1-kg AVO28 crystal.

There are vacancies without unpaired electrons that cannot be detected by EPR. At present, it is difficult to estimate the concentrations of these vacancies. However, we believe that the comparison of EPR signals in a dark environment and under illumination reveals a significant portion of vacancy defects.

Substitutional nitrogen atoms in a silicon crystal ($Si_4 \equiv N\bullet$) were identified using EPR by Murakami *et al.* [28] and Sprenger *et al.* [29]. However, in our experiment, the EPR signal of nitrogen impurity, which was considered to be contained in the AVO28 crystal with a relatively high concentration, was not detected. This can be explained by the geometrical structure of atoms determined by Jones *et al.* [30], where most of the nitrogen atoms in silicon crystals exist in the form of interstitial atoms without unpaired electrons ($Si_3 \equiv N$:, where the colon sign symbolizes a lone pair of electrons).

To the best of our knowledge, vacancies captured by nitrogen impurities have not been identified using EPR. They are not listed in the collected EPR data of the 415 types of defects in silicon [13].

Abe *et al.* [31] observed an FZ silicon crystal after copper decoration using X-ray topography. They reported that the vacancy concentration has a maximum value at the center of the radial direction of the crystal. The sample used in our EPR measurement was located near the rim of the AVO28 crystal. We need to perform an EPR measurement on the sample near the center of the crystal to obtain additional results in the near future.

VI. Conclusion

For the future realization of the kilogram using the XRCD method, it is essential to ensure the reliability of the mass deficit correction for vacancy defects. Therefore, we conducted quantitative EPR measurements on ^{28}Si single crystal AVO28 at 25 K both in a dark environment and under illumination. The following conclusions were obtained.

1) Isotropic EPR spectra from phosphorus impurity and defects near the mechanically damaged surfaces were observed. The concentration of phosphorus impurity in the AVO28 crystal was determined to be $3.2(5) \times 10^{12}$ cm^{-3} under illumination, which was consistent with that estimated using FTIR spectroscopy, $10(10) \times 10^{12}$ cm^{-3}.
2) Anisotropic EPR signals of vacancy defects in the AVO28 crystal were not observed. This demonstrates that the concentrations of the nine types of vacancy defects in the silicon crystal with unpaired electrons, which were identified in previous EPR studies, were less than the detection limit of our EPR measurement, around 1×10^{12} cm^{-3}.
3) As a result, the mass deficit correction due to the nine types of vacancy defects was estimated to be 0.0(2) μg for 1-kg AVO28 spheres.

Acknowledgment

Several parts of the sample preparation process were conducted in the clean room for analog–digital superconductivity (CRAVITY) at the National Institute of Advanced Industrial Science and Technology and MicroNano Open Innovation Center of Micromachine Center.

References

[1] *Consultative Committee for Mass and Related Quantities, Mise en Pratique of the Definition of the Kilogram in the SI, Ver. 11.3*. Accessed: Nov. 9, 2018. [Online]. Available: http://www.bipm.org/
[2] R. D. Deslattes and E. G. Kessler, "The molar volume of silicon: Discrepancies and limitations," *IEEE Trans. Instrum. Meas.*, vol. 48, no. 2, pp. 238–241, Apr. 1999.
[3] J. Gebauer, F. Rudolf, A. Polity, R. Krause-Rehberg, J. Martin, and P. Becker, "On the sensitivity limit of positron annihilation: Detection of vacancies in as-grown silicon," *Appl. Phys. A, Solids Surf.*, vol. 68, no. 4, pp. 411–416, Apr. 1999.
[4] G. D'Agostino, M. Di Luzio, G. Mana, L. Martino, M. Oddone, and C. P. Sasso, "Quantification of the void volume in single-crystal silicon," *Anal. Chem.*, vol. 88, no. 23, pp. 11678–11683, Oct. 2016.
[5] B. Andreas *et al.*, "Counting the atoms in a ^{28}Si crystal for a new kilogram definition," *Metrologia*, vol. 48, no. 2, pp. S1–S13, Mar. 2011.
[6] G. D. Watkins, "A review of EPR studies in irradiated silicon," in *Proc. 7th Int. Conf. Phys. Semiconductors*, Paris, France, 1964, pp. 97–113.
[7] S. Mizushima, K. Fujii, and T. Umeda, "Electron paramagnetic resonance study on a ^{28}Si single crystal for the future realization of the kilogram," in *Proc. CPEM*, Paris, France, Jul. 2018, pp. 1–2.
[8] P. J. Mohr, D. B. Newell, and B. N. Taylor, "CODATA recommended values of the fundamental physical constants: 2014," *Rev. Mod. Phys.*, vol. 88, no. 3, p. 035009, Sep. 2016.
[9] H. A. Jahn and E. Teller, "Stability of polyatomic molecules in degenerate electronic states. I—Orbital degeneracy," *Proc. Roy. Soc. London A*, vol. 161, no. 905, pp. 220–235, Jul. 1937.

[10] Y.-H. Lee and J. W. Corbett, "EPR study of defects in neutron-irradiated silicon: Quenched-in alignment under <110>-uniaxial stress," *Phys. Rev. B, Condens. Matter*, vol. 9, no. 10, pp. 4351–4361, May 1974.
[11] G. D. Watkins, "An EPR study of the lattice vacancy in silicon," *J. Phys. Soc. Jpn.*, vol. 18, pp. 22–27, Mar. 1963.
[12] T. Umeda, S. Hagiwara, M. Katagiri, N. Mizuochi, and J. Isoya, "A Web-based database for EPR centers in semiconductors," *Phys. B, Condens. Matter*, vols. 376–377, pp. 249–252, Apr. 2006.
[13] C. A. J. Ammerlaan *et al.*, "Paramagnetic centers in silicon," in *Landolt-Börnstein Group III Condensed Matter*, vol. 41A2α. Berlin, Germany: Springer-Verlag, 2002, pp. 244–308.
[14] Y.-H. Lee and J. W. Corbett, "EPR studies in neutron-irradiated silicon: A negative charge state of a nonplanar five-vacancy cluster (V_5^-)," *Phys. Rev. B, Condens. Matter*, vol. 8, no. 6, pp. 2810–2826, Sep. 1973.
[15] A. Kawasuso, M. Hasegawa, M. Suezawa, S. Yamaguchi, and K. Sumino, "Annealing processes of vacancies in silicon induced by electron irradiation: Analysis using positron lifetime measurement," *Mater. Sci. Forum*, vols. 175–178, pp. 423–426, Jan. 1995.
[16] Y. Azuma *et al.*, "Improved measurement results for the Avogadro constant using a ^{28}Si-enriched crystal," *Metrologia*, vol. 52, no. 2, pp. 360–375, Mar. 2015.
[17] G. Feher, "Sensitivity considerations in microwave paramagnetic resonance absorption techniques," *Bell Syst. Tech. J.*, vol. 36, no. 2, pp. 449–484, Mar. 1957.
[18] J. R. Harbridge, G. A. Rinard, R. W. Quine, S. S. Eaton, and G. R. Eaton, "Enhanced signal intensities obtained by out-of-phase rapid-passage EPR for samples with long electron spin relaxation times," *J. Magn. Reson.*, vol. 156, no. 1, pp. 41–51, May 2002.
[19] S. Mizushima, M. Ueki, and K. Fujii, "Mass measurement of 1 kg silicon spheres to establish a density standard," *Metrologia*, vol. 41, no. 2, pp. S68–S74, Mar. 2004.
[20] T. F. Ciszek, T. Wang, T. Schuyler, and A. Rohatgi, "Some effects of crystal growth parameters on minority carrier lifetime in float-zoned silicon," *J. Electrochem. Soc.*, vol. 136, no. 1, pp. 230–234, Jan. 1989.
[21] R. Brunetti, C. Jacoboni, F. Nava, L. Reggiani, G. Bosman, and R. J. J. Zijlstra, "Diffusion coefficient of electrons in silicon," *J. Appl. Phys.*, vol. 52, no. 11, pp. 6713–6722, Nov. 1981.
[22] R. C. Fletcher, W. A. Yager, G. L. Pearson, and F. R. Merritt, "Hyperfine splitting in spin resonance of group V donors in silicon," *Phys. Rev.*, vol. 95, no. 3, pp. 844–845, Aug. 1954.
[23] G. Feher, "Electron spin resonance experiments on donors in silicon. I. Electronic structure of donors by the electron nuclear double resonance technique," *Phys. Rev. J. Arch.*, vol. 114, no. 5, pp. 1219–1244, Jun. 1959.
[24] G. K. Walters and T. L. Estle, "Paramagnetic resonance of defects introduced near the surface of solids by mechanical damage," *J. Appl. Phys.*, vol. 32, no. 10, pp. 1854–1859, Oct. 1961.
[25] R. A. Weeks, "The many varieties of E' centers: A review," *J. Non-Crystalline Solids*, vol. 179, pp. 1–9, Nov. 1994.
[26] G. Bartl *et al.*, "A new ^{28}Si single crystal: Counting the atoms for the new kilogram definition," *Metrologia*, vol. 54, no. 5, pp. 693–715, Oct. 2017.
[27] W. B. Jackson, D. K. Biegelsen, R. J. Nemanich, and J. C. Knights, "Optical absorption spectra of surface or interface states in hydrogenated amorphous silicon," *Appl. Phys. Lett.*, vol. 42, no. 1, pp. 105–107, Jan. 1983.
[28] K. Murakami, K. Masuda, Y. Aoyagi, and S. Namba, "Experimental tests of non-thermal effect for pulsed-laser annealing by time-resolved reflectivity and EPR measurements," *Phys. B+C*, vol. 116, nos. 1–3, pp. 564–569, Feb. 1983.
[29] M. Sprenger, E. G. Sieverts, S. H. Müller, and C. A. J. Ammerlaan, "Electron paramagnetic resonance of a nitrogen-related centre in electron irradiated silicon," *Solid State Commun.*, vol. 51, no. 12, pp. 951–955, Sep. 1984.
[30] R. Jones, S. Öberg, F. B. Rasmussen, and B. B. Nielsen, "Identification of the dominant nitrogen defect in silicon," *Phys. Rev. Lett.*, vol. 72, no. 12, pp. 1882–1885, Mar. 1994.
[31] T. Abe, H. Harada, and J. Chikawa, "Swirl defects in float-zoned silicon crystals," *Phys. B+C*, vol. 116, nos. 1–3, pp. 139–147, Feb. 1983.

Shigeki Mizushima was born in Toyama, Japan, in 1972. He received the B.S. and M.S. degrees in physics from The University of Tokyo, Tokyo, Japan, in 1995 and 1997, respectively.

He is currently with the National Metrology Institute of Japan, National Institute of Advanced Industrial Science and Technology, Tsukuba, Japan. His current research interests include electron paramagnetic resonance study on silicon crystals, mass measurement using a mass comparator, and gravity measurement using an absolute gravimeter.

Naoki Kuramoto was born in Sagamihara, Japan, in 1971. He received the B.S., M.S., and Ph.D. degrees in chemistry from Saga University, Saga, Japan, in 1993, 1995, and 1998, respectively.

From 1995 to 1998, he was a Research Fellow with the Japan Society for the Promotion of Science, Tokyo, Japan, (DC1, for doctoral course student). From 1998 to 1999, he was with the Tokyo University of Agriculture and Technology, Tokyo, in the field of physical acoustics. In 1999, he joined the National Metrology Institute of Japan/the National Institute of Advanced Industrial Science and Technology (formerly, the National Research Laboratory of Metrology), Tsukuba, Japan, where he is currently the Group Leader of the Mass Standards Group. He has developed an optical interferometer to measure the volume of ^{28}Si-enriched spheres by optical frequency tuning to lead the new definition of the kilogram based on the Planck constant. His current research interests include laser interferometry and mass standards.

Dr. Kuramoto is a member of the Japan Society of Applied Physics, the Chemical Society of Japan, and the Society of Instrument and Control Engineers.

Kenichi Fujii received the B.E., M.E., and Ph.D. degrees from Keio University, Yokohama, Japan, in 1982, 1984, and 1997, respectively. His doctoral dissertation focused on the absolute measurement of the density of silicon crystals.

In 1984, he joined the National Metrology Institute of Japan (formerly, the National Research Laboratory of Metrology), Tsukuba, Japan. In 1988, he started an absolute measurement of the density of silicon crystals for the determination of the Avogadro constant. He developed a scanning-type optical interferometer for measuring the diameter of the silicon sphere. From 1994 to 1996, he was a Guest Researcher with the Electricity Division, National Institute of Standards and Technology, Gaithersburg, MD, USA, where he was involved in the watt balance experiment. He is currently the Prime Senior Researcher with the Research Institute for Engineering Measurement, Tsukuba.

Dr. Fujii is the member of the CODATA Task Group on Fundamental Constants and the Consultative Committee for Units of the International Committee on Weights and Measures. He serves as the Coordinator for the International Avogadro Coordination Project and the Chairperson for the Working Group on Density and Viscosity of the Consultative Committee for Mass and Related Quantities.

Takahide Umeda received the B.E., M.E., and Ph.D. degrees from the University of Tsukuba, Tsukuba, Japan, in 1994, 1996, and 1999, respectively. His Ph.D. dissertation focused on localized electronic states in solar-cell materials studied by electron spin resonance (ESR) spectroscopy.

From 1998 to 1999, he was a Doctoral and a Post-Doctoral Fellow with the Japan Society of Promotion of Science, where he investigated ESR spectroscopy on crystalline silicon surfaces. From 1999 to 2003, he was a Researcher with the Fundamental Research Laboratory and Silicon Systems Research Laboratory, NEC Corporation, Tsukuba, Japan. Since 2003, he has been an Associate Professor with the University of Tsukuba, Tsukuba, Japan, where he has been a Faculty of Pure and Applied Sciences since 2010. His current research interests include magnetic resonance spectroscopy on defects and impurities in semiconductors and semiconductor devices, e.g., silicon and its large-scale integrated circuits, silicon carbide and its power transistors, gallium nitride, and diamond.